



HAL
open science

Sedimentary markers in the Provençal Basin (western Mediterranean): a window into deep geodynamic processes

Estelle Leroux, Daniel Aslanian, Marina Rabineau, Maryline Moulin, Didier Granjeon, Christian Gorini, Laurence Droz

► To cite this version:

Estelle Leroux, Daniel Aslanian, Marina Rabineau, Maryline Moulin, Didier Granjeon, et al.. Sedimentary markers in the Provençal Basin (western Mediterranean): a window into deep geodynamic processes. *Terra Nova*, 2015, 27 (2), pp.122-129. 10.1111/ter.12139 . hal-01136100

HAL Id: hal-01136100

<https://hal.sorbonne-universite.fr/hal-01136100>

Submitted on 26 Mar 2015

HAL is a multi-disciplinary open access archive for the deposit and dissemination of scientific research documents, whether they are published or not. The documents may come from teaching and research institutions in France or abroad, or from public or private research centers.

L'archive ouverte pluridisciplinaire **HAL**, est destinée au dépôt et à la diffusion de documents scientifiques de niveau recherche, publiés ou non, émanant des établissements d'enseignement et de recherche français ou étrangers, des laboratoires publics ou privés.

1
2
3
4
5
6
7
8
9
10
11
12
13
14
15
16
17
18
19
20
21
22
23
24
25
26

**Sedimentary markers in the Provençal Basin (western Mediterranean):
a window into deep geodynamic processes**

E. Leroux^{(1,3)*}, D. Aslanian⁽²⁾, M. Rabineau⁽³⁾, M. Moulin⁽²⁾, D. Granjeon⁽⁴⁾, C. Gorini⁽¹⁾, L. Droz⁽³⁾

- 1. UPMC, Univ. Paris 06, UMR 7193, ISTEP, F-75005, Paris, France
- 2. IFREMER, Centre de Brest, GM, BP 70, 29280 Plouzané, France
- 3. CNRS, UMR6538, Domaines Océaniques, IUEM-UBO, 29280 Plouzané, France
- 4. IFP-Energies Nouvelles, 4 Avenue du Bois Préau, 92852 Rueil-Malmaison

*Corresponding Author: stll.leroux@gmail.com

Abstract

Deep Earth dynamics impact so strongly the surface geologic processes that we should use sediment paleo-markers as a window into deeper earth. Derived from climate and tectonic erosive actions on the continents and related to eustasy, subsidence and isostasy, the sediment in the deep basin represents the main recorder of these processes. Nevertheless, defining and quantifying the relative role of parameters interacting in the final sedimentary architecture is not a simple task. Using a 3D-grid of seismic and wide-angle data, drillings and numerical stratigraphic modelling, we propose here a quantification of the post-rift vertical movements of the Provence Basin (West Mediterranean) with three domains of subsidence: seaward tilting on the platform and slope and purely vertical in the deep basin. These domains fit with the deeper crustal domains highlighted by previous geophysical data. The post-break-up sedimentary markers may therefore be used to identify the initial hinge lines of the rifting phase and the subsidence laws.

27

28 **Keywords:** stratigraphy, sedimentary marker, geodynamic, subsidence, passive margin

29

30 **INTRODUCTION**

31 Whilst the link between deep Earth dynamics and surface geologic processes appears more
32 and more as a key parameter, deep Earth research, encompassing fields such as seismology
33 and mantle geodynamics, has traditionally operated distinctly from fields focusing on surface
34 dynamics, such as sedimentology and geomorphology [Cloetingh *et al.*, 2013]. Nevertheless,
35 the formation of passive continental margins -namely the process by which the continental
36 lithosphere thins and subsides that remains one of the main challenges in Earth Science-,
37 allows recording in its sedimentary layers the main steps of the Earth dynamic processes
38 (subsidence, uplift, erosion, paleoclimate...). Passive margins represent a sink for sediments
39 resulting from climate and tectonic erosive actions on the continents. Sedimentary layers also
40 record the effects of eustasy, subsidence and isostasy, so that sediment appears as a storyteller
41 of the Earth.

42 We present here a quantification of the post-rift vertical movements of the Provence Basin
43 (West Mediterranean) based on the interpretation of sedimentary paleomarkers using a large
44 3D grid of seismic data, correlations with existing drillings, refraction data and validation by
45 numerical stratigraphic modelling with Dionisos [Granjeon & Joseph, 1999]. The results of
46 this 3D analysis emphasize the strong link between deep Earth dynamic processes and surface
47 geologic processes.

48

49 **Geological Setting**

50 The Provence Basin reveals a structure and evolution corresponding to a young pair of rifted
51 margins formed by the counter-clockwise rotation of the Corso–Sardinian micro-blocks with

52 respect to the Ibero–European plate from the Late Eocene (Priabonian, 33.7 Ma), in a general
53 context of collision between Africa and Europe (Figure 1-A). The opening took place at the
54 southern end of the intra-European rift system, in a back-arc situation, in response to SE
55 rollback of the slab of the African plate subducting beneath the European plate during an
56 extensional phase. This Corso–Sardinian micro-continent rotation resulted in the
57 emplacement of oceanic crust, starting in the Late Aquitanian (23 Ma to 19 Ma) and ending in
58 the Langhian (about 15 Ma) [Olivet, 1996].

59 Thanks to its recent history, the subsidence in the Provence Basin is still underway at present
60 and continually creates a large amount of space which favours a progressive filling that
61 preserves the record of both the comings and goings of shorelines associated with the rise and
62 fall of sea levels as well as the vertical movements of the margin [Rabineau *et al.*, 2005]. This
63 fact, together with the substantial seismic database available on the Provence margin,
64 including conventional standard seismic lines, high-resolution multi-channel data, very high-
65 resolution profiles and industrial drillings make this basin ideal for constraining evolutionary
66 and subsidence models of rifted continental margins using the sedimentary record.

67

68 **DATA AND METHODS**

69 Many global, regional and local factors have long been recognised to control the overall
70 geometry and deposition of sediments but defining and quantifying the relative part of
71 parameters interacting to produce the final sedimentary architecture of basins (subsidence,
72 eustasy, sediment supply) is not a simple task. This has been one of the main goals of Seismic
73 and Sequence Stratigraphy, as developed in the late 70's [Mitchum and Vail, 1977;
74 Posamentier, 1988a]. At the same time, the development of quantitative techniques for
75 geological analysis of sedimentary basins (geohistory analysis) were developed [Van Hinte,
76 1978; Jervey, 1988 ; Allen and Allen, 1990 ; Robin *et al.*, 1996]. They aim to produce a curve

77 for subsidence and sediment accumulation rates through time. This is reached after a number
78 of corrections (decompaction, paleobathymetry and absolute sea-level fluctuations) based on
79 available datasets. The total subsidence is therefore partitioned into contributions from
80 tectonic driving forces, thermal evolution, sediment loading and sea-level fluctuations
81 [Steckler and Watts, 1978 ; Allen & Allen, 2005]. This backstripping depends on strong
82 assumptions: the isostatic response of the lithosphere (e.g. Airy vs regional flexure),
83 theoretical law for porosity, paleobathymetries, sea-level changes, densities of mantle and
84 crust and thermal subsidence. Moreover, lateral and longitudinal variations along a margin are
85 important and 1D modeling cannot be applied to the entire margin.

86 Rabineau *et al.* [2014] presented a new method to quantify the post-rift subsidence by the
87 direct use of sedimentary geometries. In this paper, we apply this method in a 3D analysis of
88 sedimentary geometries. In a first step, seismic stratigraphy and borehole data have been used
89 to interpret and date the paleosurfaces on all profiles. Those have been correlated at a regional
90 scale and converted in depth using ESP and sonic data from wells to generate isobath and
91 isopach maps and to quantify sediment fluxes through time [Leroux, 2012]. In a second step,
92 10 fictitious regional lines were extracted from this set of isobath maps (Figure 1-B). We then
93 built vertical dip and strike sections in order to quantify the 3D vertical evolution and
94 potential tectonic deformation of the margin. On each profile, we adjusted paleosurfaces to
95 straight lines, to measure their subsidence rates (Figure 1-C). This method highlights not only
96 the evolution of subsidence through time but also its spatial segmentation along the margin.

97

98 **QUANTIFICATION OF SUBSIDENCE**

99 For each profile, three domains of different subsidence were identified by dips and slope-
100 breaks of each horizon¹ (Figure 1-C). Subsidence on the shelf is characterised by a Plio-
101 Quaternary tilt of $0.16^\circ/\text{Myr}$ about a rotational axis located 15 km landward of the present-
102 day coastline (Hinge Line 1, HL1). This Plio-Quaternary subsidence is constant through time
103 [Leroux *et al.*, 2014]. During the Miocene, this rate varies spatially: $0.12^\circ/\text{Myr}$ on the western
104 sections and $0.06^\circ/\text{Myr}$ on the eastern sections, using the same hinge line 1.

105 Seawards of the hinge line 3 (HL3), in the distal part of the margin, Miocene and Plio-
106 Quaternary reflectors are flat and parallel to the substratum, indicating a purely vertical
107 subsidence. The strong early erosion at the top of the synrift deposits or directly on the
108 substratum suggests a subaerial position of the substratum before the first post-rift deposit
109 [Bache *et al.*, 2010]. This erosional surface is observed on the entire margin and allows us to
110 consider a high position of the entire margin (with a paleobathymetry above sea-level) at the
111 end of rifting. Considering an age of 20 Ma for the end of rifting [Séranne, 1999], we can then
112 calculate the mean post-rift vertical subsidence rate in the deep basin of 500 m/Myr.

113 Between these two domains, the slope accommodates vertical movements of either side.
114 Whilst the slope break between the slope and the deep basin (hinge line 3) is fixed in space
115 through time, the hinge line 2 (HL2) between the shelf and the slope varies during the
116 Pliocene within an area of less than 20 km, which mainly reflects the prograding-aggrading

¹ Plio-Quaternary key reflectors labelled MES (Margin Erosional Surface in pink), P11 (yellow), PXX (turquoise-blue), Q10 (red), Q5 (purple) and seafloor (marine-blue) are respectively dated at 5.33 Ma, 2.6 Ma, 1.6 Ma, 0.9 Ma, 0.5 Ma and 0 Ma [Leroux *et al.*, 2014]. The substratum (brown) and Miocene markers such as the base of the MSC (Messinian Salinity Crisis in red), the base of Mb -interpreted as an evaporitic unit- (orange), the base and top of salt (green and light green) and the top of UU (Upper Unit in grey) are from [Bache *et al.*, 2009].

117 sedimentary system on the shelf [Rabineau *et al.*, 2014] rebuilding the margin after the
118 Messinian erosional event [Lofi *et al.*, 2003].

119 This 3D quantification of subsidence in three domains was then tested with Dionisos
120 [Granjeon and Joseph, 1999] using the quantitative constraints on sediment supply inferred
121 from a 3D stratigraphic analysis (Leroux, 2012, Leroux *et al.*, 2014, [Fig S1. in Supplementary](#)
122 [Material](#)) and the eustatic curve of Haq *et al.*, (1987), modified by a 1500 m drawdown during
123 the MSC [Clauzon *et al.*, 1982] ([Fig S1. in Suppl. Material](#)).

124 [Figure 2](#) demonstrates that the 3D modelling successfully restores the stratigraphic record
125 with the sedimentary geometries and thicknesses observed from seismic data. This modelling
126 is coherent with micropaleontological data from Miocene borehole samples on the shelf
127 [Cravatte *et al.*, 1974] that reveals a deepening of the depositional environment at this time
128 ([see Figures S1, S2, S3 and movies S4, S5, S6 in Suppl. Material](#)). The aggrading shelf-slope
129 geometries during the Early to Middle Miocene indicate that the morphology of the margin
130 and the subsidence pattern changed after this early erosion and led to the creation of
131 accommodation. After rifting, the entire Gulf of Lions margin was thus affected by strong
132 post-rift subsidence leading to thick post-rift (Miocene to Quaternary) sedimentary
133 accumulations. After the MSC we can observe a Pliocene progradation trend followed by a
134 Pleistocene progradation-aggradation trend (after 2.6 Ma). All these elements are well
135 reproduced by our simulation.

136 Western Mediterranean basins and margins have undergone a transition into Late Neogene
137 basin inversion (e.g. Roure *et al.*, 2013). Increase in the level of intraplate compression in the
138 Northern Atlantic region could explain the observed rapid phases of Plio-Quaternary
139 subsidence after a phase of quiescence [Cloetingh & Kooi, 1992]. Moreover, in the Gulf of
140 Lion, sediment flux during Pliocene (after 5.33 Ma) is 3 times higher than the flux in the
141 Miocene ([Figure S1 in Suppl. Material](#)). This increasing sediment load, driven by climate or

142 tectonic, may therefore play an important role in the increasing subsidence. However, since
143 2004, many studies on passive margins, which are not in back-arc setting nor in inversion,
144 have shown delayed subsidence which increases long after the breakup, as on Spitzberg
145 Margin [Ritzmann, *et al.*, 2004], on Iberia-Newfoundland Margins [Peron-Pinvidic &
146 Manatschal, 2008], on Morocco Margin [Labails *et al.*, 2009], on Brazilian margins [Aslanian
147 *et al.*, 2009], on Angola margin [Moulin *et al.*, 2005] or on the Gulf of Lion margin [Bache *et*
148 *al.*, 2010; Aslanian *et al.*, 2012; Moulin *et al.*, in press]. In some margins, the presence of
149 carbonates overlying the salt layer shows that a shallow environment lasted after the break-up.
150 The subsidence rate then seems to increase rapidly. The general character of the delayed
151 subsidence followed by an increased subsidence rate implies probably a deep contribution like
152 a lithosphere driven process (as proposed by Aslanian *et al.*, 2009; Huismans & Beaumont,
153 2011, 2014; Aslanian *et al.*, 2012), without excluding basin inversion process and/or
154 sediment overloading”.

155

156 **CORRELATION WITH THE UNDERLYING CRUSTAL DOMAINS**

157 Four structural domains extending from the coast to the oceanic crust have been highlighted
158 on the basis of gravity, magnetic, reflection and wide-angle seismic data (Figure 3) [Pascal *et*
159 *al.*, 1993, Gailler *et al.*, 2009, Aslanian *et al.*, 2012, Moulin *et al.*, in press; Afilhado *et al.*, in
160 press]: a) a 20 km thick continental crust (thinned crust), b) a highly thinned continental zone
161 (the continental necking zone as described by Kooi *et al.*, 1992 ; Cloetingh *et al.*, 1995),
162 which is marked by a prominent reflector (T) easily recognised at depth [De Voogd *et al.*,
163 1991 ; Moulin *et al.*, in press], c) a 5 km thin domain of unknown crust and complex nature
164 (called a transitional domain), and last d) a thin oceanic crust. The limit between the necking
165 and the transitional domains corresponds to the French-side limit of the pre-rift
166 paleogeography [Olivet, 1996]. The base of the necking and transitional domains presents a 4

167 km thick layer with anomalous seismic velocities (6.8 – 7.5 km/s) which are neither typical of
168 continental crust nor oceanic crust [Pascal *et al.*, 1993, Gailler *et al.*, 2009 ; Moulin *et al.*, in
169 press, Afilhado *et al.*, in press.]. The nature of the transitional domain was a matter of debate
170 [De Voogd *et al.*, 1991; Pascal *et al.*, 1993 ; Séranne, 1999 ; Gailler *et al.*, 2009 ; Bache *et al.*,
171 2010 ; Aslanian *et al.*, 2012] but the recent results of wide-angle seismic analysis seem in
172 favour of an exhumed lower continental crust nature [Moulin *et al.*, in press; Afilhado *et al.*,
173 in press]. This is beyond the scope of this paper, but a consensus does exist on the very
174 different nature of this crust compared to the crustal domains observed on both sides, and the
175 transitional crust may have different physical behaviour.

176 [Figure 3](#) presents our reconstructed 3D subsidence map and the striking correlation between
177 the three differential subsidence domains described using paleo-markers and the underlying
178 crustal domains highlighted by geophysical data. Up to present day, the crustal limits defined
179 by the passive margin genesis still control, at the very first order, the vertical movements
180 recorded by sedimentary sequences.

181

182 Not all passive margins exhibit a sag basin, with a « pure » vertical subsidence. Therefore, the
183 use of depositional architecture can give a first approximation for the partitioning of the
184 subsidence (with or without a sag basin) and the basement surface geometry.

185 In the GOL, the sag basin is described to be allochthonous, with exhumed lower crust near the
186 necking and anomalous thinned oceanic crust in the middle of the basin [Aslanian *et al.*,
187 2012; Moulin *et al.*, in press; Afilhado *et al.*, in press]. This partitioning, with different
188 magnetic and gravity patterns, fits the palaeogeographic reconstructions and is also observed
189 in the salt geometry (connected /separated domes).

190

191 Using wide-angle and reflection seismic data, a similar observation was made for the Angola
192 Margin, where the sag basin exhibits a similar mainly vertical, pre-breakup and post-breakup

193 subsidence [Moulin *et al.*, 2005; Aslanian *et al.*, 2009]. As shown in the Gulf of Lion, the
194 post-break-up subsidence of the Angolan basin uses the same hinge lines that have built and
195 segmented the passive margin [Moulin *et al.*, 2005]. However, the nature of its basement is
196 different from the GOL, with an autochthonous upper continental crust (just after the necking)
197 and an allochthonous crust that can be exhumed or intruded [Moulin *et al.*, 2005; Aslanian *et*
198 *al.*, 2009]. This partitioning is also observed in the salt geometry (connected/separated
199 domes), and fits the initial palaeogeographic reconstruction [Moulin *et al.*, 2010; Aslanian &
200 Moulin, 2010; 2012].

201 The difference between the two examples shows that a sag basin can occur with different
202 crustal nature as shown by geophysical data. In both cases the exhumed/intruded lower
203 continental crust is involved. The wide angle results in GOL [Afilhado *et al.*, in press] and in
204 the Santos Basin [Klingelhoefer *et al.*, 2015; Evain *et al.*, accepted] show that the transition
205 between exhumed lower crust to oceanic crust is not abrupt and raises the question on the role
206 of the lower continental crust “flow“, that can be gradually recrystallized to build the first
207 atypical oceanic crust [Bott, 1971; Aslanian *et al.*, 2009; Sibuet *et al.*, 2012; Evain *et al.*,
208 accepted; Afilhado *et al.*, in press].

209 Anyway, in both cases, whilst the combination of depositional architecture, surface
210 observations and palaeogeographic reconstructions will not give the exact crustal nature, they
211 can give crucial information such as: basement surface geometry,
212 allochthonous/autochthonous nature, and, thanks to magnetism, oceanic nature.

213

214 **CONCLUSION**

215 Using the new method of Rabineau *et al.* [2014] to quantify the post-rift subsidence by the
216 direct use of sedimentary geometries on the 3D analysis of tilts of stratigraphic markers in the
217 Gulf of Lions margin, we individualize three domains of subsidence: on the platform and

218 slope, the subsidence takes the form of a seaward tilting with different amplitudes, whereas
219 the deep basin subsides purely vertically, as in the case of a sag basin. These domains fit with
220 the deeper crustal domains highlighted by previous geophysical data implying that the post-
221 break-up subsidence re-uses the initial hinge lines of the rifting phase and that the
222 sedimentary record (even the last 5 Ma) is correlated with the underlying structural domains.
223 This study provides therefore strong evidence for the recognition and importance of the link
224 between deep Earth dynamic processes and surface geological processes [e.g. Braun, 2010,
225 Cloetingh *et al.*, 2013]. The vertical coupling between mantle and surface processes promises
226 new insights into past mantle dynamics through the geological record and the sediments are a
227 precious tool for deciphering the laws of subsidence, even in their recent history, and can be
228 considered as the storyteller of vertical and horizontal movements (Rabineau, 2014) and can
229 be used as a window on deep geodynamic processes.

230

231 **ACKNOWLEDGEMENTS**

232 Stratigraphic simulations were performed with IFP-Energies Nouvelles Dionisos software
233 kindly made available to the University of Brest. This research was mainly funded by CNRS
234 and IFREMER, with additional support from the French Actions-Marges program (JL Rubino
235 & P. Unternehr) and the GRI “Méditerranée” (Groupement Recherche et Industrie). This
236 work also benefited from the Labex Mer initiative, a State Grant from the French Agence
237 Nationale de la Recherche (ANR) in the Program « Investissements d'avenir » with the
238 reference ANR-10-LABX-19-01, Labex Mer. The authors are grateful to Katalin Kovacs for
239 post-editing the English style. We also thanks Jim Pindell and an anonymous reviewer for
240 their very fruitful comments that greatly improved this paper, as well as Max Coleman,
241 Scientific Editor and the anonymous associated editor for their reading and encouragements.

242

243 **Competing financial interests**

244 The authors declare no competing financial interests.

245

246 **FIGURE CAPTIONS**

247 Fig1. (A) Location of the study area (black box) on a bathymetric map of the Provence Basin.

248 Opening of the basin is illustrated by black arrows. Shaded area corresponds to the oceanic

249 crust domain. (B) Location of all our synthetic vertical sections on our bathymetric map

250 drawn from seismic data (B). This map also shows the extension of our stratigraphic

251 interpretation and the position (red line) of the dip section shown on (C) in which the tilts and

252 the subsidence of stratigraphic paleosurfaces are analysed. Colored circles correspond to

253 slope-breaks for each of these surfaces. Three hinge-lines (grey area) are noted. On the shelf

254 these stratigraphic surfaces allowed us to measure a constant Plio-Quaternary subsidence tilt

255 rate ($0.16^\circ/\text{Myr}$). The tilt rate of the substratum is $0.11^\circ/\text{Myr}$ if we denote the end of rifting at

256 20 Ma. In the basin, the post-rift subsidence is purely vertical; its mean rate is estimated at

257 around 500 m/Myr (see the text for explanation).

258

259 Figure 2. (A) Deposit paleobathymetries and resultant geometries predicted by Dionisos in

260 our 3D stratigraphic modelling of the Gulf of Lion and Provence basin. The sedimentary

261 architecture of the margin and final depths of the stratigraphic markers (relative to the

262 substratum) are well reproduced by the model. We can compare this simulation with the NW-

263 SE seismic profile ECORS 1 on (B): on both we observe the deepening of the Miocene

264 depositional environment, the Messinian trilogy (LU, MU & UU after Lofi et al., 2011) and

265 the prograding trend during the Pliocene followed by a prograding-aggrading trend during the

266 Pleistocene (after 2.6 Ma). Note that the vertical scale units are respectively metres in A and

267 seconds (twtt) in B. This explains the relative differences in unit thicknesses, in particular for

268 the pre-Messinian Miocene unit. See also seismic lines corresponding to the black boxes S1 &
269 S2 in the supplementary information.

270

271 Figure 3. (A) 3D post-rift subsidence map drawn after our seismic interpretation and the
272 analyses of our 10 synthetic vertical sections. The structural domains highlighted by
273 geophysical data [Moulin et al., in press] and the geometries of the post-rift sedimentary pile
274 are reported along a NW-SE dip line-drawing (B). There exists a striking correlation between
275 the sedimentary record of subsidence and the nature of the underlying crust. The continental
276 crust (domains 1 and 2) is tilted whereas the intermediate COT (Continent-Ocean Transition)
277 domain (domain 3) subsides in a purely vertical way, such as in a sag basin. See the text for
278 explanation.

279

280 **SUPPLEMENTARY MATERIAL**

281 • Figure S1. Major input parameters (evolution of the eustatic curve and sediment supply) for
282 the 3D simulation of post-rift filling of the Provence basin. The simulation was run over the
283 last 20 Ma with a 0.1 Ma time-step. The basin is defined as a rectangular area (250x400 km)
284 and the initial basement at 20 Ma is flat with a paleobathymetry around +100 m (cf text for
285 explanation).

286

287 • Figure S2. Interpreted LRM18 seismic reflection profile. The offlap-breaks are represented
288 with white dots; Inset: the overall geometry of Pliocene-Quaternary strata shows prograding
289 clinoforms (or prisms) with a clear geometrical change in the Late Pliocene to Quaternary
290 clinoforms (after yellow horizon p11), from essentially prograding (green) to prograding-
291 aggrading (yellow). Leroux *et al.*, 2014 (in press).

292

293 • Figure S3. Comparison between (A) a regional seismic profile from (Bache, 2009) and (B)
294 the same seismic profile extracted by Dionisos from our Messinian modelling. On this
295 synthetic seismic line, the impedance contrasts (in red and blue scale) highlight the same
296 discontinuities we have observed on the seismic profile A. The final simulated present-day
297 topography (in blue-scale) is superimposed on the synthetic section.

298

299 • Movie S4. 3D stratigraphic model of the Gulf of Lions and Provence basin from 20 to 0 Ma.
300 The movie shows deposit paleobathymetries and resultant geometries predicted by Dionisos.

301

302 • Movie S5. Evolutional model of the Gulf of Lions and Provence basin through 3D
303 stratigraphic modelling during the Messinian Salinity Crisis. The movie shows deposit
304 paleobathymetries and resultant geometries predicted by Dionisos.

305

306 • Movie S6. Evolutional model of the Gulf of Lions and Provence basin through 3D
307 stratigraphic modelling during the Messinian Salinity Crisis. The movie shows lithologic
308 facies and resultant geometries predicted by Dionisos.

309

310

311 REFERENCES CITED

312

313 Afilhado, A., Moulin, M., Klingelhoefer, F., Aslanian, D., Schnurle, P., Nouzé, H., Rabineau, M. & Beslier,
314 M.O., in press. Deep crustal structure across an young passive margin from wide-angle and reflection seismic
315 data (The SARDINIA Experiment) - II. Sardinia's margin, BSGF, ILP Special volume, in press.

316 Allen, P. and Allen, J., 1990. Basin analysis, Principles and Applications (Blackwell Publishing Ltd, 1st Edition,
317 1990), 451 pp.

318 Allen, P. and Allen, J., 2005. Basin analysis, Principles and Applications (Blackwell Publishing Ltd, Second
319 Edition), 549 pp.

- 320 Aslanian, D., Moulin, M., Olivet, J.-L., Unternehr, P., Matias, L., Bache, F., Rabineau, M., Nouzé, H.,
321 Klingelhoefer, F., 2009. Brazilian and african passive margins of the central segment of the south atlantic ocean:
322 Kinematic constraints, *Tectonophysics*, 468, 98–112.
- 323 Aslanian, D. & Moulin, M., 2010. Comments on «A new scheme for the opening of the south Atlantic Ocean
324 and the dissection of an Aptian salt Basin» from Torsvik et al, 2009. *Geophys. J. Int.* 183, 20-28.
325 doi:10.1111/j.1365-246X.2010.04727.x.
- 326 Aslanian, D. & Moulin, M., 2012. Paleogeographic consequences of conservational models in the South Atlantic
327 Ocean. In: W.U. Mohriak, A. Danforth, P.J. Post, D.E. Brown, G.C. Tari, M. Nemcok, S.T. Sinha (Eds.),
328 *Conjugate Divergent Margins*, Geological Society, London, Special Publications, 369.
- 329 Aslanian, D., Rabineau, M., Moulin, M., Schnurle, P., Klingelhoefer, F., Gailler, A., Bache, F., Leroux, E.,
330 Gorini, C., Droxler, A., Eguchi, N., Kuroda, J., Alain, K., Roure, F. & Haq, 2012. Structure and evolution of the
331 Gulf of Lions: the Sardinia seismic experiment and the GOLD (Gulf of Lions Drilling) project. *Leading Edge*.
- 332 Bache, F., Olivet, J.-L., Gorini, C., Rabineau, M., Baztan, J., Aslanian, D., Suc, J.-P., 2009. Messinian erosional
333 and salinity crisis: View from the Provence basin (Gulf of Lions, Western Mediterranean). *Earth and Planet. Sci.*
334 *Lett.*, 286, 139–157.
- 335 Bache, F., Olivet, J.-L., Gorini, C., Aslanian, D., Labails, C. and Rabineau, M., 2010. Evolution of rifted
336 continental margins : The case of the gulf of lions (western mediterranean basin), *Earth and Planet. Sci. Lett.*,
337 292, 345–356.
- 338 Bott, M.P.H., 1971. Evolution of young continental margins and formation of shelf basins. *Tectonophysics*, 11
339 (5), 319-327.
- 340 Braun, J., 2010. The many surface expressions of mantle dynamics. *Nature Geosci.* 3, 825-833.
- 341 Clauzon, G., 1982. Le canyon messinien du rhône : une preuve décisive du dessiccated deep-basin model. *Bull.*
342 *Soc. Geol. France* 24, 597–610.
- 343 Cloetingh, S. & Kooi, H., 1992. Tectonics and global change –inferences from Late Cenozoic subsidence and
344 uplift patterns in the Atlantic/Mediterranean region. *Terra Nova (Global Change Spec. Issue)*, 4, 340-350.
- 345 Cloetingh, S., van Wees, J.D., van der Beek, P.A., Spadini, G., 1995. Role of pre-rift rheology in kinematics of
346 extensional basin formation: constraints from thermomechanical models of Mediterranean and intracratonic
347 basins. *Mar. Petrol. Geol.* 12 (8), 793-807.
- 348 Cloetingh, S. & Willett, S.D., 2013. TOPO-EUROPE: Understanding of the coupling between the deep Earth
349 and continental topography. *Tectonophysics*, 602, 1-14.

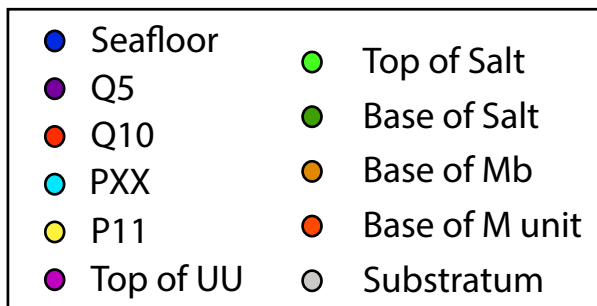
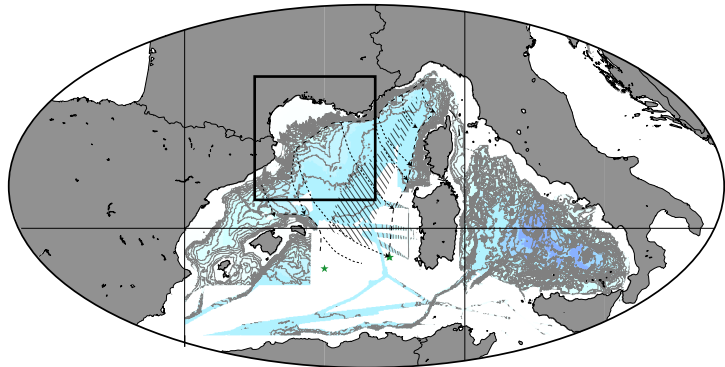
- 350 Contrucci, I., Matias, L., Moulin, M., Géli, L., Klingelhoefer, F., Nouzé, H., Aslanian, D., Olivet, J.-L., Sibuet,
351 J.-C., Réhault, J.-P., 2004. Deep structure of the west african continental margin, between 5°s and 8°s, from
352 reflection/refraction seismics and gravity data, *Geophys. J. Int.*, 158, 529–553.
- 353 Cravatte, J., Dufaure, P., Prim, M., Rouaix, S., 1974. Les sondages du golfe du lion : Stratigraphie,
354 sédimentologie, Compagnie Française des Pétroles, Paris.
- 355 De Voogd, B., Nicolich, R., Olivet, J.L., Fanucci, F., Burrus, J., Mauffret, A., Pascal, G., Argnani, A., Auzende,
356 J.M., Bernabini, M., Bois, C., Carmignani, L., Fabbri, A., Finetti, I., Galdeano, A., Gorini, C.Y., Labaume, P.,
357 Lajat, D., Patriat, P., Pinet, B., Ravat, J., Ricci Lucchi, F., Vernassa, S., 1991. First deep seismic reflection
358 transect from the Gulf of Lions to Sardinia (ECORS-CROP profiles in Western Mediterranean). In: Meissner, R.
359 (Ed.), *Continental Lithosphere: Deep seismic reflections*. American Geophysical Union, 265-274.
- 360 Evain, M., Afilhado, A., Rigoti, C., Loureiro, A., Alves, D., Klingelhoefer, F., Schnurle, P., Feld, A., Fuck, R.,
361 Soares, J., Vinicius de Lima, M., Corela, C., Matias, L., Benabdellouahed, M., Baltzer, A., Rabineau, M., Viana,
362 A., Moulin, M., Aslanian, D. (accepted). Deep structure of the Santos Basin-Sao Paulo Plateau System, SE
363 Brazil. *J. Geophys. Research*, xx, xx-xx.
- 364 Gailler, A., Klingelhoefer, F., Olivet, J.-L., Aslanian, D., the Sardinia scientific party, and T. O. team, 2009.
365 Crustal structure of a young margin pair: new results accross the liguro-provencal basin from wide-angle seismic
366 tomography. *Earth and Planet. Sci. Lett.*, 286, 333–345.
- 367 Granjeon, D., Joseph, P., 1999. Concepts and applications of a 3-d multiple lithology, diffusive model in
368 stratigraphic modelling. In: *Numerical Experiments in Stratigraphy:Recent Advances in Stratigraphic and*
369 *Sedimentologic Computer Simulation*, SEPM Spec. Pub. 62, Tulsa, 197–210.
- 370 Haq, B.U., Hardenbol, J., Vail, P., 1987. Chronology of fluctuating sea levels since the Triassic (250 million
371 years ago to present). *Sci.*, 235, 1156-1167.
- 372 Huismans, R. & Beaumont, C., 2011. Depth-dependant extension, two-stage breakup and cratonic underplating
373 at rifted margins. *Nature*, 473, 74-79.
- 374 Huismans, R. & Beaumont, C., 2014. Rifted continental margins: the case for depth-dependent extension. *Earth*
375 *and Planet. Sci. Lett.*, 407, 148-162.
- 376 Jervey, M.T., 1988. Quantitative geological modelling of siliclastic rock sequences and their seismic
377 expressions, in: Wilgus, C.K., Hastings, B.S., St Kendall, C.G., Ross, C.A., Van Wagoner, J.C. (Eds.), *Sea-level*
378 *changes: an integrated approach*. SEPM Special Publication, Tulsa, pp. 47-69.

- 379 Klingelhoefer, F., Evain, M., Afilhado, A., Rigoti, C., Loureiro, A., Alves, D., Leprêtre, A., Moulin, M.,
380 Schnurle, P., Benabdellouahed, M., Baltzer, A., Rabineau, M., Feld, A., Viana, A., Aslanian, D., 2015. Imaging
381 proto-oceanic crust off the Brazilian Continental Margin. *Geophys. J. Int.*, 200 (1), 471-488.
- 382 Kooi, H., Cloetingh, S., Burrus, J., 1992. Lithospheric Necking and Regional Isostasy at Extensional Basins. 1.
383 Subsidence and Gravity Modeling with an Application to the Gulf of Lions margin (SE France). *J. of Geophys.*
384 *Research*, 97(B12), 17553-17571.
- 385 Labails, C. & Olivet J.-L. & the Dakhla study group, 2009. Crustal structure of the SW Moroccan margin from
386 wide-angle and reflection data (the Dakhla experiment). Part B., The tectonic heritage. *Tectonophysics*, 468 (1-
387 4), 83-97.
- 388 Leroux, E., 2012 Quantification des flux et de la subsidence du bassin Provençal (Méditerranée occidentale).
389 PhD, Université de Bretagne Occidentale, 457 pp. <http://archimer.ifremer.fr/doc/00108/21967/20279.pdf>
- 390 Leroux, E., Rabineau, M., Aslanian, D., Gorini, C., Droz, L., Granjeon, D., 2014. Stratigraphic simulation on the
391 shelf of the Gulf of Lions : testing subsidence rates and sea-level curves during Pliocene and Quaternary, *Terra*
392 *Nova*, doi: 10.1111/ter.12091.
- 393 Lofi, J., Rabineau, M., Gorini, C., Berné, S., Clauzon, G., Clarens, P. D., Reis, A. D., Mountain, G. S., Ryan,
394 W., Steckler, M., Fouchet, C., 2003. Plio-quaternary prograding clinoform wedges of the Western Gulf of Lion
395 continental margin (NW Mediterranean) after the messinian salinity crisis, *Mar. Geol.*, 198, 289–317.
- 396 Lofi, J., Sage, F., Deverchère, J., Loncke, L., Maillard, A., Gaullier, V., Thinon, I., Gillet, H., Guennoc, P.,
397 Gorini, C., 2011. Refining our knowledge of the Messinian Salinity crisis records in the offshore domaine
398 through multi-site seismic analysis. *Bull. Soc. Géol. Fr.*, 182, 163-180.
- 399 Moulin, M., Aslanian, D., Olivet, J.-L., Contrucci, I., Matias, L., Géli, L., Klingelhoefer, F., Nouzé, H., Rehault,
400 J.P., Untemehr, P., 2005. Geological constraints on the evolution of the angolan margin based on reflection and
401 refraction seismic data (ZaiAngo project). *Geophys. J. Int.*, 162, 793-818.
- 402 Moulin, M., Aslanian, D., Unternehr, P., 2010. A new starting point for the South and Equatorial Atlantic Ocean,
403 *Earth-Science Reviews*, 98(1-2), 1-37.
- 404 Moulin, M., Klingelhoefer, F., Afilhado, A., Feld, A., Aslanian, D., Schnurle, P., Nouzé, H., Rabineau, M.,
405 Beslier M.O., in press. Deep crustal structure across a young passive margin from wide-angle and reflection
406 seismic data (the sardinia experiment) - I. Gulf of Lions margin.. *BSGF, ILP Special volume*.
- 407 Mitchum, R.M., Vail, P.R., Thompson, S., 1977a. Seismic stratigraphy and global changes of sea level, part 2:
408 the depositional sequence as a basic unit for stratigraphic analysis, in: Payton, C.E. (Ed.), *Seismic stratigraphy -*

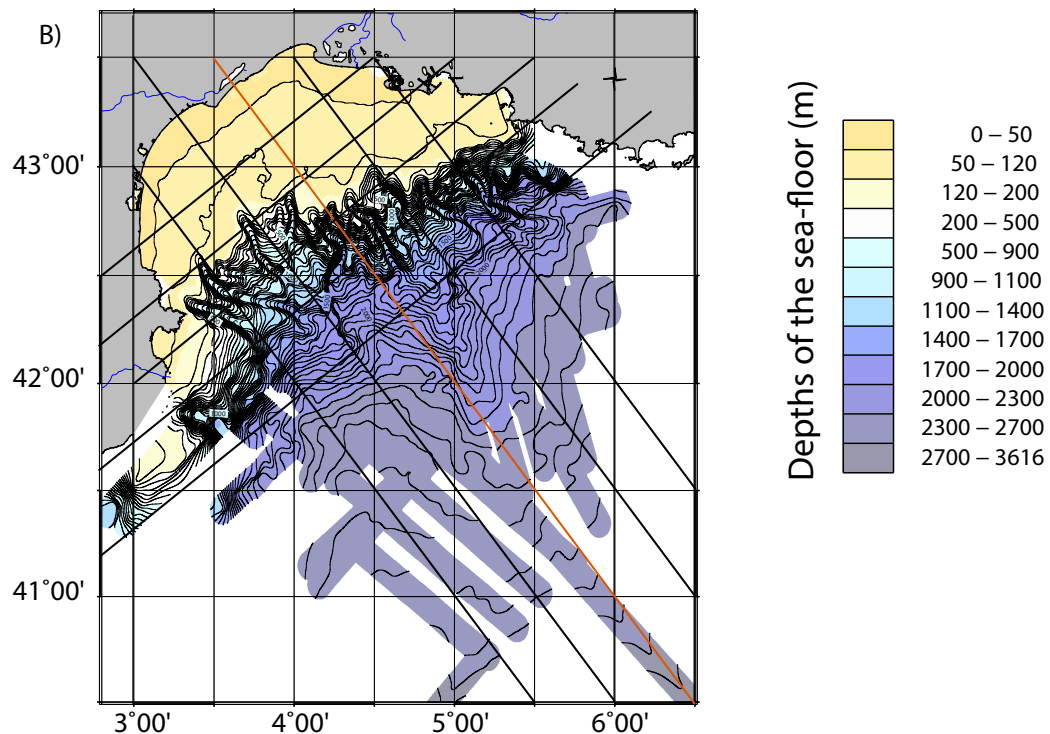
- 409 Application to hydrocarbon exploration. AAPG Mem. 26, Tulsa, Oklahoma, pp. 53-62.
- 410 Olivet, J.-L., 1996. La cinématique de la plaque ibérique, Bulletin du Centre de Recherche et d'Exploration,
411 Production Elf Aquitaine, 20, 131–195.
- 412 Pascal G., Mauffret, A., Patriat, P., 1993. The ocean-continent boundary in the Gulf of Lions from analysis of
413 expanding spread profiles and gravity modelling. *Geophys. J. Int.* 113, 701-726
- 414 Peron-Pinvidic, G. & Manatschal, G., 2008. The final rifting evolution at deep magma-poor passive margins
415 from Iberia-Newfoundland: a new point of view. *Int. J. Earth Sci. (Geol Rundsch)*, 98, 1581-1597. DOI
416 10.1007/s00531-008-0337-9.
- 417 Posamentier, H.W., Jervey, M.T., Vail, P.R., 1988a. Eustatic controls on clastic deposition I. Conceptual
418 framework, in: Wilgus, C.K., Hastings, B.S., Kendall, C.G.S.C., Posamentier, H.W., Ross, C.A., Van Wagoner,
419 J.C. (Eds.), *Sea-Level Changes- an Integrated Approach*. SEPM Spec. Pub. 42, Tulsa, pp. 102-124.
- 420 Rabineau, M., Berné, S., Aslanian, D., Olivet, J.-L., Joseph, P., Guillocheau, F., Bourillet, J.-F., Le Drezen, E.,
421 Granjeon, D., 2005. Sedimentary sequences in the gulf of lions : A record of 100,000 years climatic cycles,
422 *Marine and Petroleum geology*, 22, 775–804.
- 423 Rabineau, M., Leroux, E., Bache, F., Aslanian, D., Gorini, C., Moulin, M., Molliex, S., Droz, L., Reis, A.D.,
424 Ritzmann, O., Jokat, W., Czuba, W., Guterch, A., Mjelde, R., Nishimura, Y., 2004. A deep seismic transect from
425 Hovgard Ridge to northwestern Svalbard across the continental-ocean transition: A sheared margin study.
426 *Geophys. J. Int.*, 157(2), 638-702.
- 427 Rubino, J.-L., Olivet, J.-L., 2014. Quantification of pliocene-quaternary subsidence and isostatic readjustment
428 related to the messinian crisis (using paleobathymetric markers in the Gulf of Lion). *Earth Planet. Sci. Lett.* 388,
429 1–14.
- 430 Robin, C., Guillocheau, F., Gaulier, J.M., 1996. Mesure des signaux eustatiques et tectoniques au sein de
431 l'enregistrement sédimentaire d'un bassin intracratonique. Application au Lias du bassin de Paris. *Comptes*
432 *Rendus de l'Académie des Sciences de Paris* 322, 1079-1086.
- 433 Roure, F.M., Casero, P., Addoum, B., 2013. Mesozoic and Cenozoic Basins Formation and Deformation along
434 the North African Margin. *Search and Discovering Article #30276, AAPG2013*.
- 435 Séranne, M., 1999. The Gulf of Lion continental margin (NW Mediterranean) revisited by IBS: an overview, in:
436 Steckler, M.S. & Watts, A.B., 1978. Subsidence of the Atlantic-type continental margin off New York. *Earth*
437 *and Planetary Science Letters*, 41 (1), 1-13.

- 438 Sibuet, J.-C. & Tucholke, B.E., 2012. The geodynamic province of transitional lithosphere adjacent to magma-
439 poor continental margins. Geol. Society, London, Special Publication, 369, 429-452.
- 440 Durand, B., Jolivet, L., Horvath, F., Seranne, M. (Eds.), The Mediterranean Basins: Tertiary Extension within
441 the Alpine Orogen. Special publication, Geological Society of London.
- 442 Van Hinte, J.E., 1978. Geohistory analysis: application of micropaleontology in exploration geology. Bull. Am.
443 Ass. Pet. Geol. 62, 201-222.
- 444
- 445
- 446

A)



B)



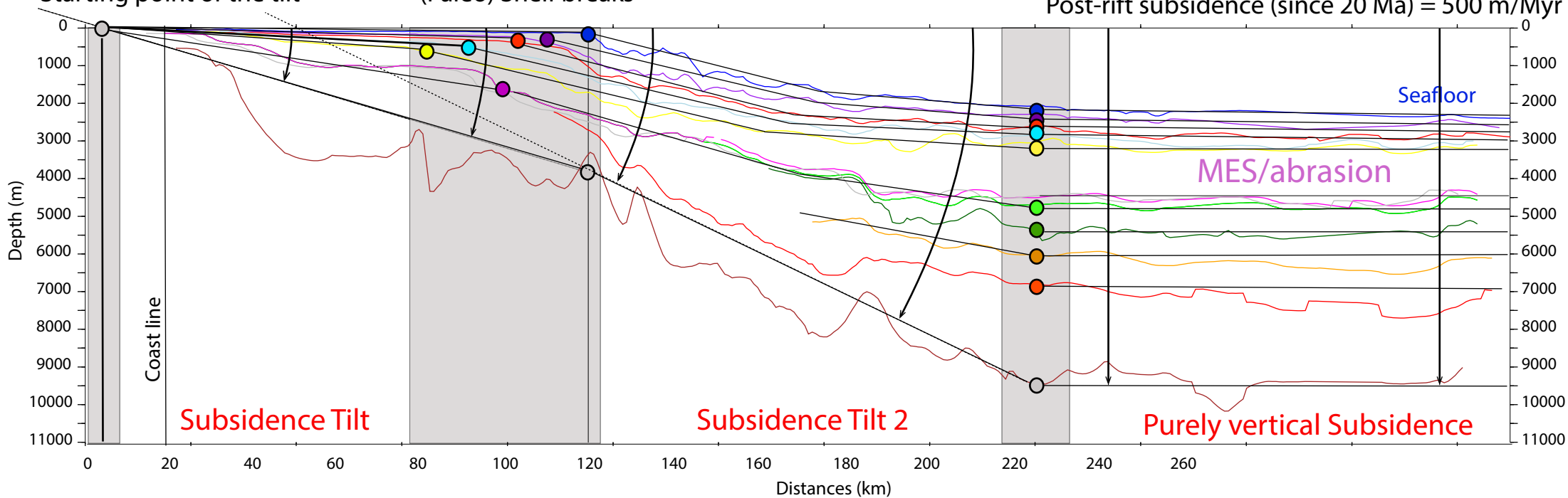
C)

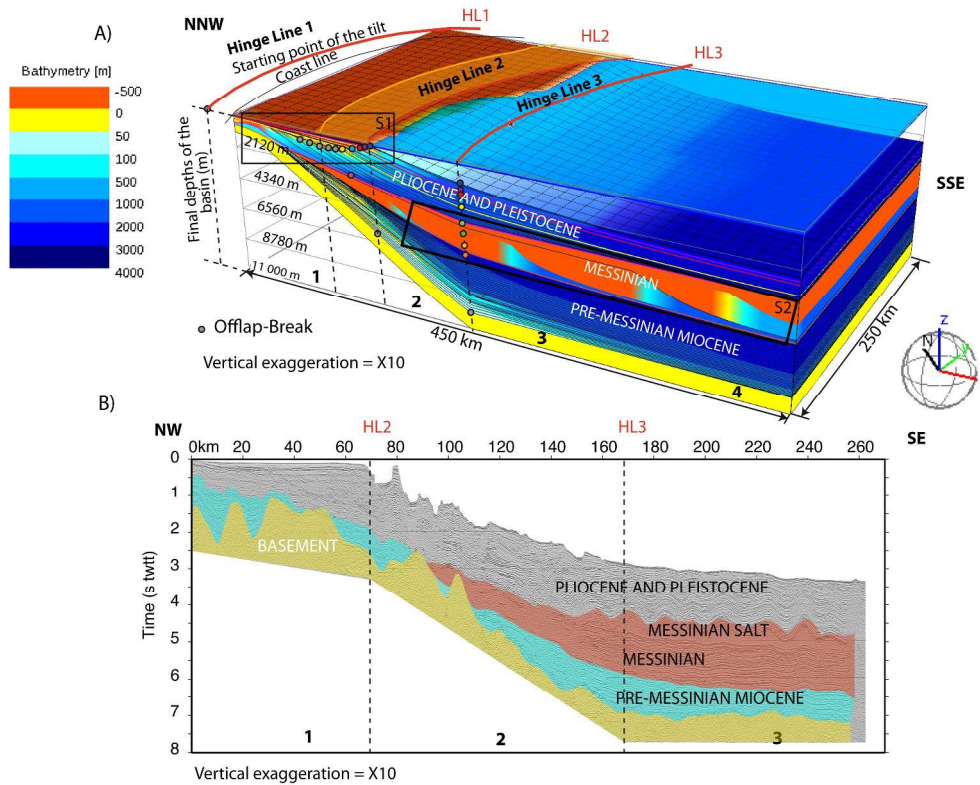
Hinge Line 1:
Starting point of the tilt

Hinge Line 2:
(Paleo) Shelf breaks

Hinge Line 3

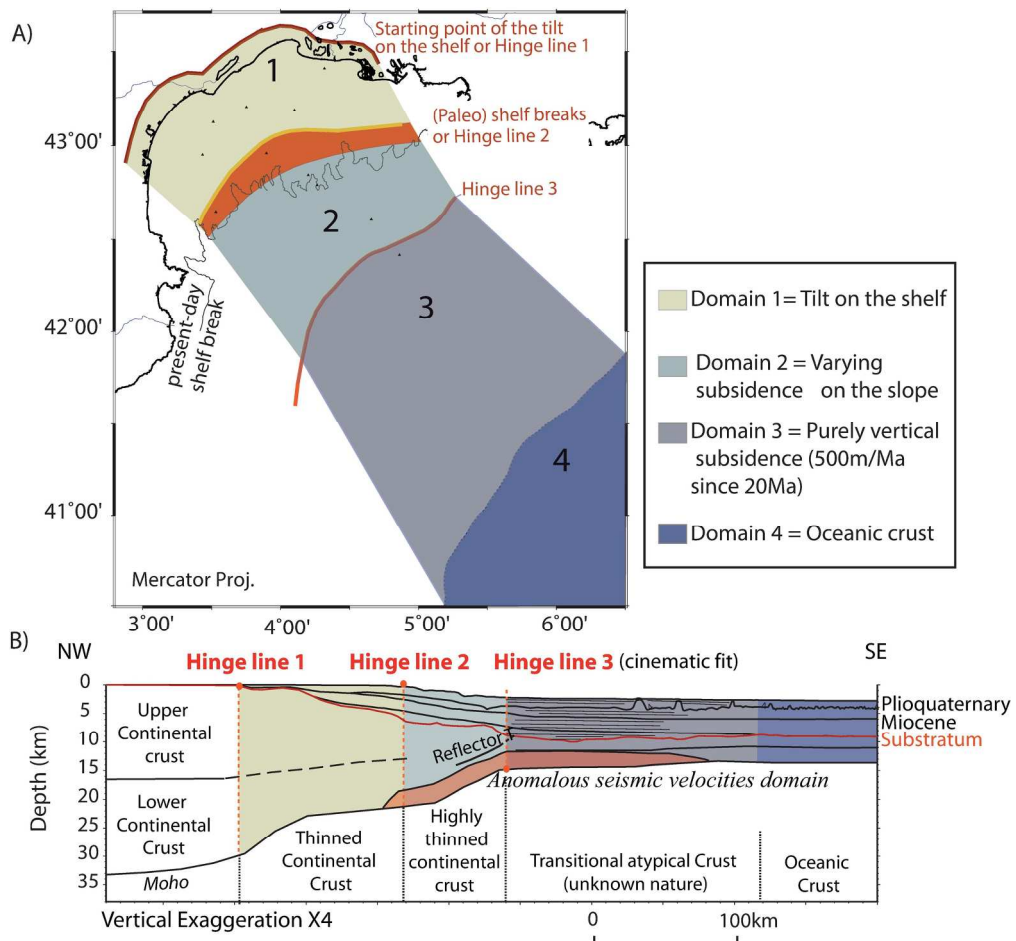
Post-rift subsidence (since 20 Ma) = 500 m/Myr





Deposit paleobathymetries and resultant geometries predicted by Dionisos in our 3D stratigraphic modelling of the Gulf of Lion and Provence basin (A). The sedimentary architecture of the margin and final depths of the stratigraphic markers (relative to the substratum) are well reproduced by the model. We can compare this simulation with the NW-SE seismic profile ECORS 1 on (B): on both we observe the deepening of the Miocene depositional environment, the Messinian trilogy and the prograding trend during the Pliocene followed by a prograding-aggrading trend during the Pleistocene (after 2.6 Ma). Note that the vertical scale units are respectively metres in A and secondes (twtt) in B. This explains the relative differences in unit thicknesses, in particular for the pre-Messinian Miocene unit. See also seismic lines corresponding to the black boxes S1 & S2 in the supplementary information.

260x205mm (300 x 300 DPI)



208x215mm (300 x 300 DPI)

Supplementary material

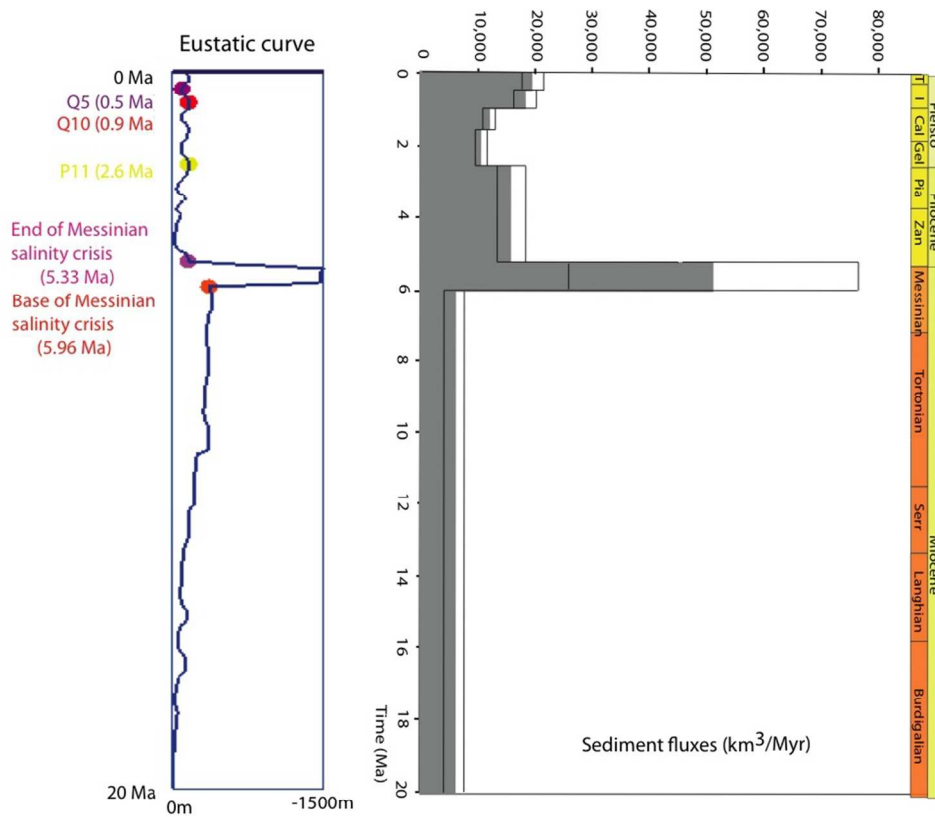
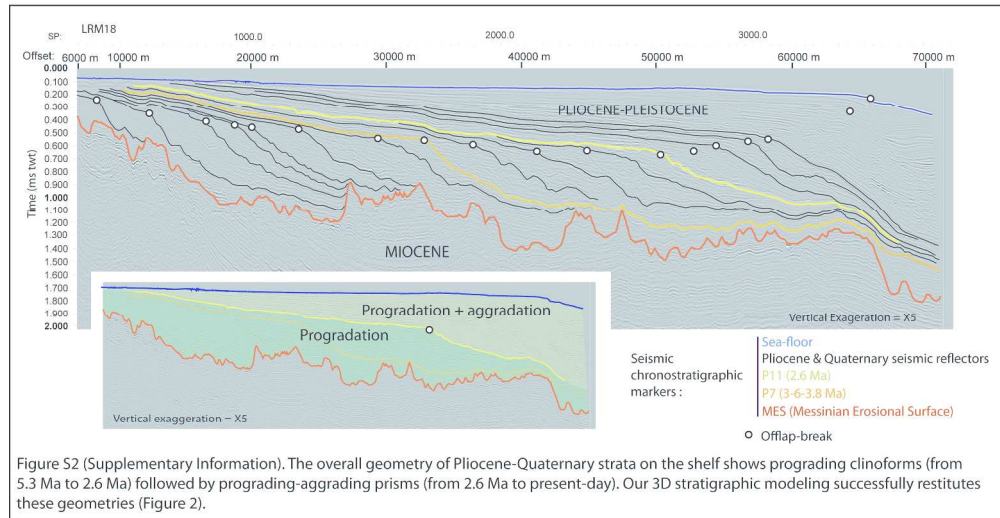


Figure S1 (Supplementary Information). Major input parameters into the model (subsidence excluded): evolution of eustatic curve and sediment supply

Major input parameters (evolution of the eustatic curve and sediment supply) for the 3D simulation of post-rift filling of the Provence basin. The simulation was run over the last 20 Ma with a 0.1 Ma time-step. The basin is defined as a rectangular area (250x400 km) and the initial basement at 20 Ma is flat with a paleobathymetry around +100 m (cf text for explanation).

173x156mm (150 x 150 DPI)



Interpreted LRM18 seismic reflection profile. The offlap-breaks are represented with white dots; Inset: the overall geometry of Pliocene-Quaternary strata shows prograding clinoforms (or prisms) with a clear geometrical change in the Late Pliocene to Quaternary clinoforms (after yellow horizon p11), from essentially prograding (green) to prograding-aggrading (yellow). Leroux et al., 2014.

1080x565mm (72 x 72 DPI)

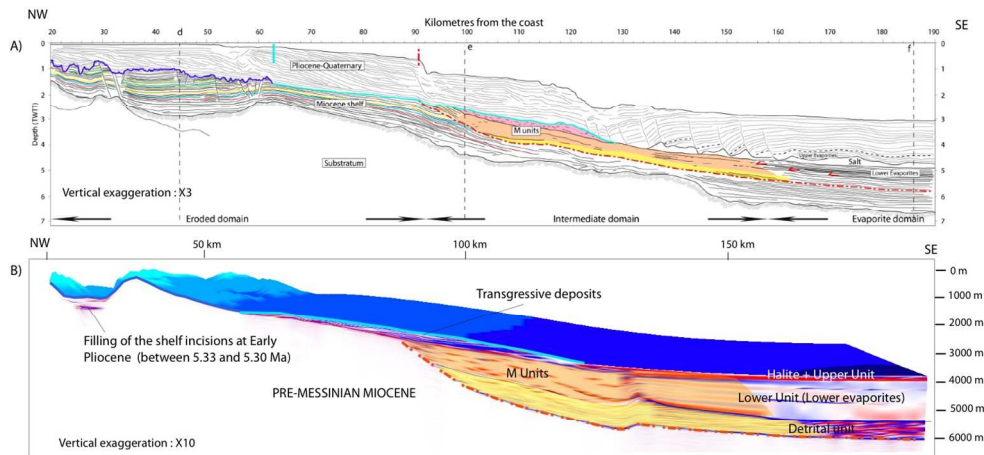


Figure S3 (Supplementary Information). Comparison between (A) a regional seismic profile and (B) the same seismic profile extracted by Dionisos from our Messinian modelling. Our 3D modelling successfully restitutes the sediment geometries during the Messinian Salinity Crisis.

Comparison between (A) a regional seismic profile from (Bache, 2009) and (B) the same seismic profile extracted by Dionisos from our Messinian modelling. On this synthetic seismic line, the impedance contrasts (in red and blue scale) highlight the same discontinuities we have observed on the seismic profile A. The final simulated present-day topography (in blue-scale as function of the depth) is surimposed on the synthetic section.

259x135mm (150 x 150 DPI)